Journal of Applied Polymer Science

Controlled electrochemical synthesis of conductive nanopolypyrrole and its application in the design of a solid-state ion sensor

Ishwar Das,[1] Namita Rani Agrawal,[2] Avinash Kumar Pandey,[1] Rinki Choudhary,[1] P. C. Pandey[3]

[1]Chemistry Department, Deen Dayal Upadhyay Gorakhpur University, Gorakhpur 273009, India
[2]Chemistry Department, St. Andrew's College, Gorakhpur 273009, India
[3]Chemistry Department, Indian Institute of Technology (BHU), Varanasi 221005, India
Correspondence to: N. R. Agrawal (E-mail: rani.namita@rediffmail.com)

ABSTRACT: A polypyrrole (PPy) conductive polymer was electrochemically synthesized from pyrrole–cupric chloride ($CuCl_2$)–H_2O (system A) and pyrrole–$CuCl_2$–sodium dodecyl sulfate–H_2O (system B). Their morphologies and growth behavior were studied, and their aggregates were characterized by powder X-ray diffraction, scanning electron microscopy, transmission electron spectroscopy, thermogravimetry, and Fourier transform infrared studies. The powder X-ray diffraction pattern showed only one peak characteristic of PPy. In system B, the dimensions of the fractal patterns were calculated and found to be very close to the theoretical value of diffusion-limited aggregation. Various morphological transitions were observed at different field intensities and $CuCl_2$ concentrations. Transmission electron spectroscopy studies revealed the formation of nanosized spherical particles 5–10 nm in size. For system B, a potassium-ion-selective electrode was constructed on the basis of a dibenzo-18-crown-6 impregnated poly(vinyl chloride) matrix membrane over a synthesized polymer-modified electrode. The electrode showed Nernstian behavior with a slope of 57 mV; this revealed the potential application of the as-synthesized material in the design of a solid-state ion-selective electrode. © 2015 Wiley Periodicals, Inc. J. Appl. Polym. Sci. **2015**, *132*, 42729.

KEYWORDS: applications; conducting polymers; copolymers; nanostructured polymers

Received 4 December 2014; accepted 12 July 2015
DOI: 10.1002/app.42729

INTRODUCTION

Polypyrrole (PPy) is one of the most promising and studied organic conductive polymers because of its good stability and conductivity.[1–3] It has wide potential applications as sensors, electric devices, and several others. It is well known that PPy films doped with electrolyte anions exhibit a high conductivity.[4] The size and morphology are two fundamental aspects of nanostructures that determine the optical, electronic, and mechanical properties of the materials.[5,6] PPy was synthesized by a solution method with different surfactants and ammonium persulfate as an oxidant.[7] It was also synthesized by the chemical oxidative polymerization of pyrrole in aqueous solution containing an oxidant ferric sulfate and a surfactant.[8] Wire, ribbon, and spherelike nanostructures of PPy have been synthesized by solution chemistry methods in the presence of various surfactants and oxidizing agents, such as ammonium persulfate or ferric chloride.[9] Various PPy–noble metal composites have been investigated;[10] these have exhibited a variety of useful optical, electrical, magnetic, and catalytic properties.[11] A new route for preparing PPy–hydroquinone nanobeads were proposed by Chen *et al.*[12] Liu *et al.*[13] synthesized a graphene/branching-like PPy/$CoFe_2O_4$ composite. The kinetics and degradation of electrical conductivity in PPy were studied by Samuelson and Druy.[14] Pina *et al.*[15] reviewed the metal-catalyzed syntheses of polyaniline and PPy conductive polymers. The morphology is an important factor that influences the characteristics and performance of conductive polymers. Fractal structures are generally observed in nonequilibrium growth processes, such as electrodeposition,[16–18] crystal growth,[19,20] electropolymerization,[21] and chemical dissolution,[22] and also in biological systems, such as bacterial growth.[23–25] The incorporation of a surfactant into a conducting PPy synthesized in the presence of copper salt is likely to improve the morphology, electrical conductivity, particle size, and ion-sensing behavior and can be used in the construction of solid-state ion-selective electrodes.[26] The desired ion carrier within the poly(vinyl chloride) (PVC) membrane matrix on to conductive PPy may lead to the design of solid-state ion-selective electrodes for potential analytical applications.[26] Dibenzo-18-crown-6 was chosen as potassium ion-sensing neutral carrier for casting over conductive PPy films to evaluate the performance of surfactant-mediated synthesized PPy-modified electrodes. Indeed, interesting findings on the ion-sensing characteristics of the as-synthesized material are reported in this article.

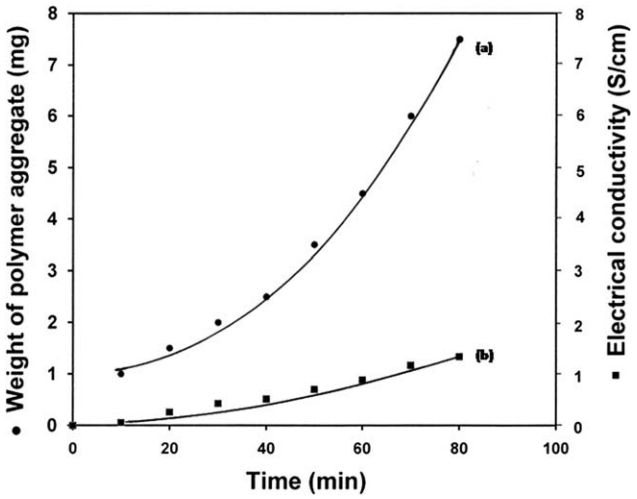

Figure 1. (a) Weight and (b) electrical conductivity of the polymer aggregates as a function of the time during the electropolymerization of pyrrole in the pyrrole–$CuCl_2{\cdot}2H_2O$–H_2O system (conditions: [pyrrole] = 0.25*M*, [$CuCl_2{\cdot}2H_2O$] = 0.025*M*, field intensity = 2.4 V/cm, separation between electrodes = 2.5 cm).

We synthesized PPy electrochemically with a less expensive cupric chloride ($CuCl_2$) in the absence and presence of an anionic surfactant, sodium dodecyl sulfate (NaDS). Its growth behavior, morphology, electrical conductivity, thermal stability, scanning electron microscopy (SEM), transmission electron spectroscopy (TEM) studies, fractal dimension (*D*) calculation, and application were studied.

EXPERIMENTAL

Pyrrole (Merck Schuchardt), $CuCl_2$ (Merck Specialties Private, Ltd.), NaDS (extrapure, S. D. Fine Chem, Ltd.), PVC powder, dibenzo-18-crown-6 (Aldrich), sodium tetraphenyl boron (SISCO, India), dibutyl phthalate (Qualigens Fine Chemicals), tetrahydrofuran (THF; Molychem), and MilliQ water were used in the experiment. The potentiometric measurements were made in 0.1*M* Tris–HCl buffer at pH 7.0 with a double-junction calomel electrode.

Electrochemical Synthesis

Polymer aggregates were obtained by the electropolymerization of pyrrole in its aqueous solution containing $CuCl_2$ (system A) and $CuCl_2$ and the anionic surfactant NaDS (system B) under different experimental conditions with an experimental setup consisting of a circular platinum cathode with a radius of 2.5 cm and a vertical anode. The vertical anode was put at the center of the circular cathode such that it touched the surface of an aqueous solution of pyrrole monomer and $CuCl_2$ placed in a Petri dish. All solutions were prepared in MilliQ water. These electrodes were attached to a potentiostat (Scientific India). The experiment was carried out under different experimental conditions. Polymerization was also carried out in the presence of the anionic surfactant NaDS.

Measurements

In system A, experiments were carried out at different time intervals, field intensities, and $CuCl_2$ concentrations. The aggregates were washed with water and dried in a vacuum desiccator. The dried aggregates were photographed and weighed. The electrical conductivity of the aggregates was measured at room temperature with an experimental setup, as described earlier.[27] The results are shown in Figures 1–3.

The influence of the anionic surfactant, NaDS, on the electrochemical polymerization of pyrrole in the presence of $CuCl_2$ was studied at different field intensities and $CuCl_2$ concentrations. The results are shown in Figures 4 and 5.

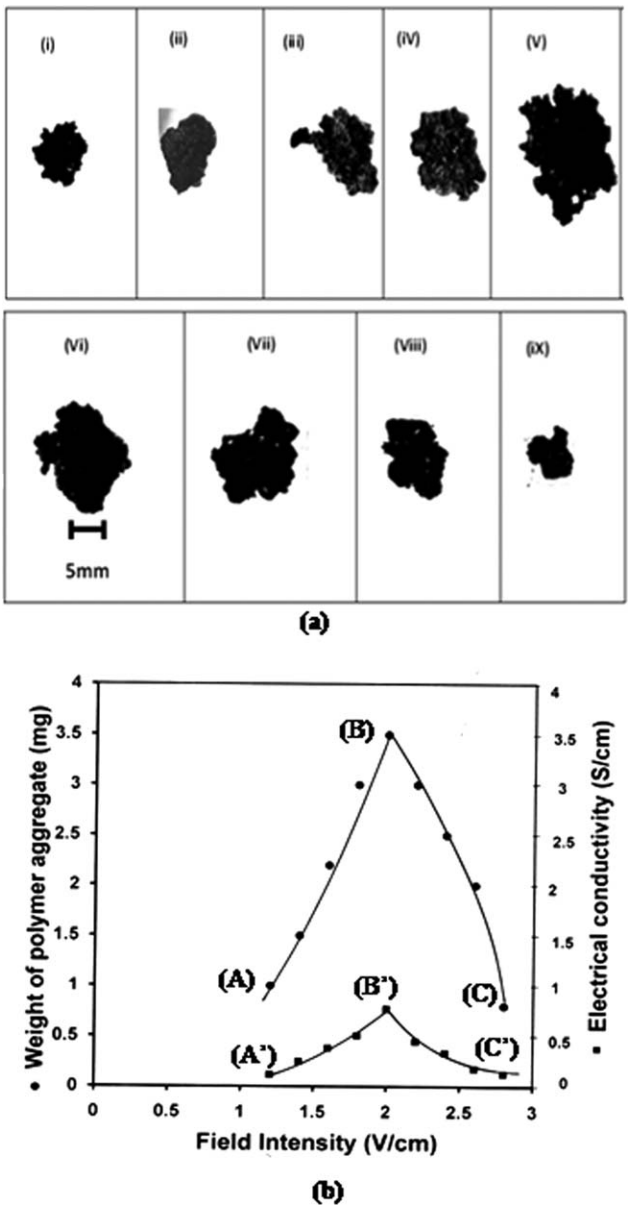

Figure 2. (a) Microphotographs and (b) plots of the weight (curve ABC) and electrical conductivity (curve A′B′C′) of the polymer aggregates as a function of the field intensity obtained during the electropolymerization of pyrrole in the pyrrole–$CuCl_2{\cdot}2H_2O$–H_2O system {conditions: [pyrrole] = 0.25*M*; [$CuCl_2{\cdot}2H_2O$] = 0.025*M*; field intensities = (i) 1.2, (ii) 1.4, (iii) 1.6, (iv) 1.8, (v) 2.0, (vi) 2.2, (vii) 2.4, (viii) 2.6, and (ix) 2.8 V/cm; duration of polymerization = 30 min; separation between electrodes = 2.5 cm}.

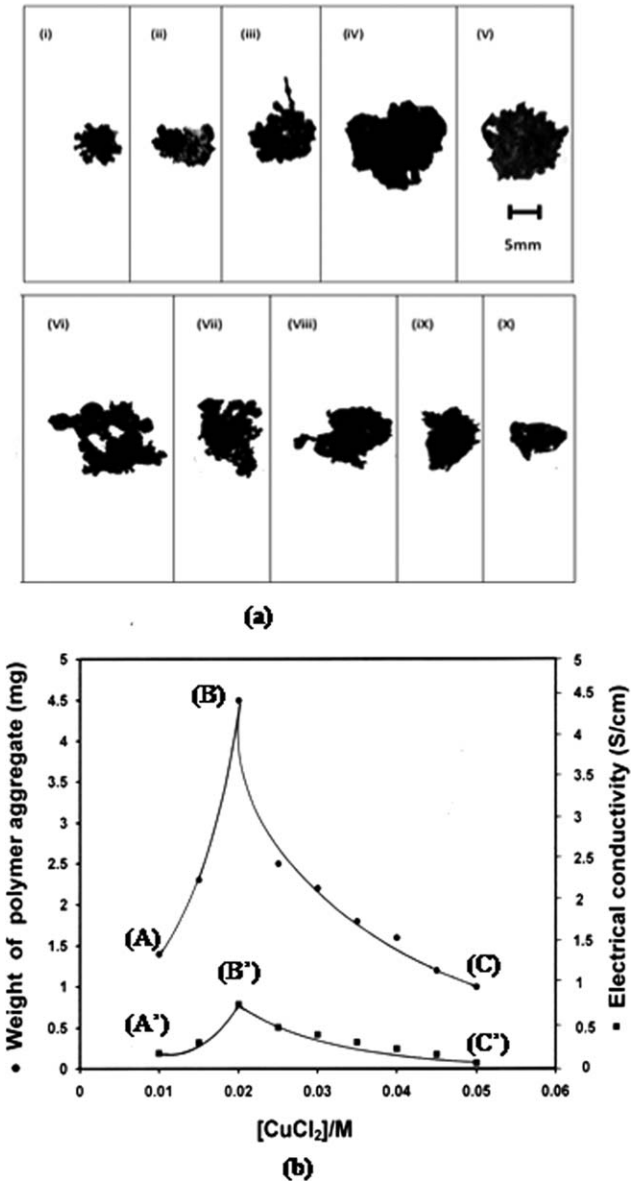

Figure 3. (a) Microphotographs and (b) plots of the weight (curve ABC) and electrical conductivity (curve A′B′C′) of the polymer aggregates as a function of the $CuCl_2{\cdot}2H_2O$ concentration obtained in the pyrrole–$CuCl_2{\cdot}2H_2O$–H_2O system {conditions: [pyrrole] = 0.25*M*; [$CuCl_2{\cdot}2H_2O$] = (i) 0.005, (ii) 0.01, (iii) 0.015, (iv) 0.02, (v) 0.025, (vi) 0.03, (vii) 0.035, (viii) 0.04, (ix) 0.045, and (x) 0.05M; field intensities = 2.4 V/cm; duration of polymerization = 30 min; separation between electrodes = 2.5 cm}.

The *D* values of the growth patterns shown in Figures 4 and 5 were calculated by a box-counting method, as described earlier.[19] The total number of pixels [$N(r)$] in a circle of radius r is related by the relationship $N(r) \sim r^D$. *D* of the fractal patterns could be obtained from the plot of log $N(r)$ versus log r with the method of least squares analysis. The results are recorded in Table I.

A powder X-ray diffraction pattern of the polymer aggregate obtained from system A was taken in the 2θ range of 10–70° from Indian Institute of Technology Delhi. The result is shown in Figure 6.

With regard to the morphological properties, SEM images of the electropolymerized aggregates obtained from both systems A and B were taken with a scanning electron microscope (model JSM-7600F). The results are shown in Figure 7. TEM images of these aggregates were also taken with a Philips transmission electron microscope (model CM 200). The results are shown in Figure 8.

To study the thermal properties, thermogravimetry (TG)/differential thermogravimetry (DTG) studies were carried out from STIC Cochin. The heating rate was maintained at 10°C/min. The results are shown in Figure 9.

The IR spectra of the polymer aggregates were taken from STIC Cochin.

Construction of a K^+-Selective Electrode

The electrode body used for the construction of the electropolymerized PPy and, subsequently, the ion sensor based on the dibenzo-18-crown-6 impregnated PVC membrane was made from a Teflon cylinder. The gold disk on the brass rod was screwed within a hollow-screwed Teflon cylinder; this resulted in an electrode body with a cavity with a recessed depth of 2 mm. The exposed diameter of the gold disk to be used as an active surface for sensor construction was 2 mm. The electropolymerization of the pyrrole was carried out in $CuCl_2{\cdot}2H_2O$ in the presence of anionic surfactant at a constant potential; this resulted in an excellent film. The electropolymerized PPy film was washed with distilled water and dried over a night at 35°C. The solution of the PVC casting membrane was made in dried THF with the following components: PVC fine powder (11.2 mg), dibenzo-18-crown-6 (1 mg), dibutyl phthalate (30 μL), sodium tetraphenyl boron (0.8 mg), and THF (300 μL).

After the complete dissolution of the membrane material, 20–30 μL of the solution was added to the recessed depth of the electrode body covered with the PPy film. The solvent (THF) was allowed to evaporate slowly over a 20-h period at room temperature. When the solvent was completely evaporated, a transparent smooth layer of the sensing membrane remained at the surface of the PPy-modified electrode. The resulting electrode was conditioned for 6–8 h in a 1*M* KCl solution.

Potentiometric Operation of the PPy-Modified Ion Sensor

The potentiometric responses of the ion sensor constructed previously were carried out in 0.1*M* Tris–HCl buffer at pH 7.0 with a double-junction calomel electrode.

The ion sensor, together with a double-junction reference electrode, was dipped in the stirred electrochemical cell with a working volume of 15 mL; the electrode potential was monitored by Keithley multimeter connected to a personal computer through an RS 232 interface. At the steady-state potentiometric response, various concentrations of the ionic solution were injected into the cell, and the new steady-state potential was recorded. The results are shown in Figure 10.

RESULTS AND DISCUSSION

The controlled electrochemical synthesis of PPy was carried out in an aqueous medium containing a pyrrole monomer and $CuCl_2$ (system A) and $CuCl_2$ and the anionic surfactant NaDS (system B). It is an effective ecofriendly route to produce PPy by metal salt in aqueous medium instead of acetonitrile, as used

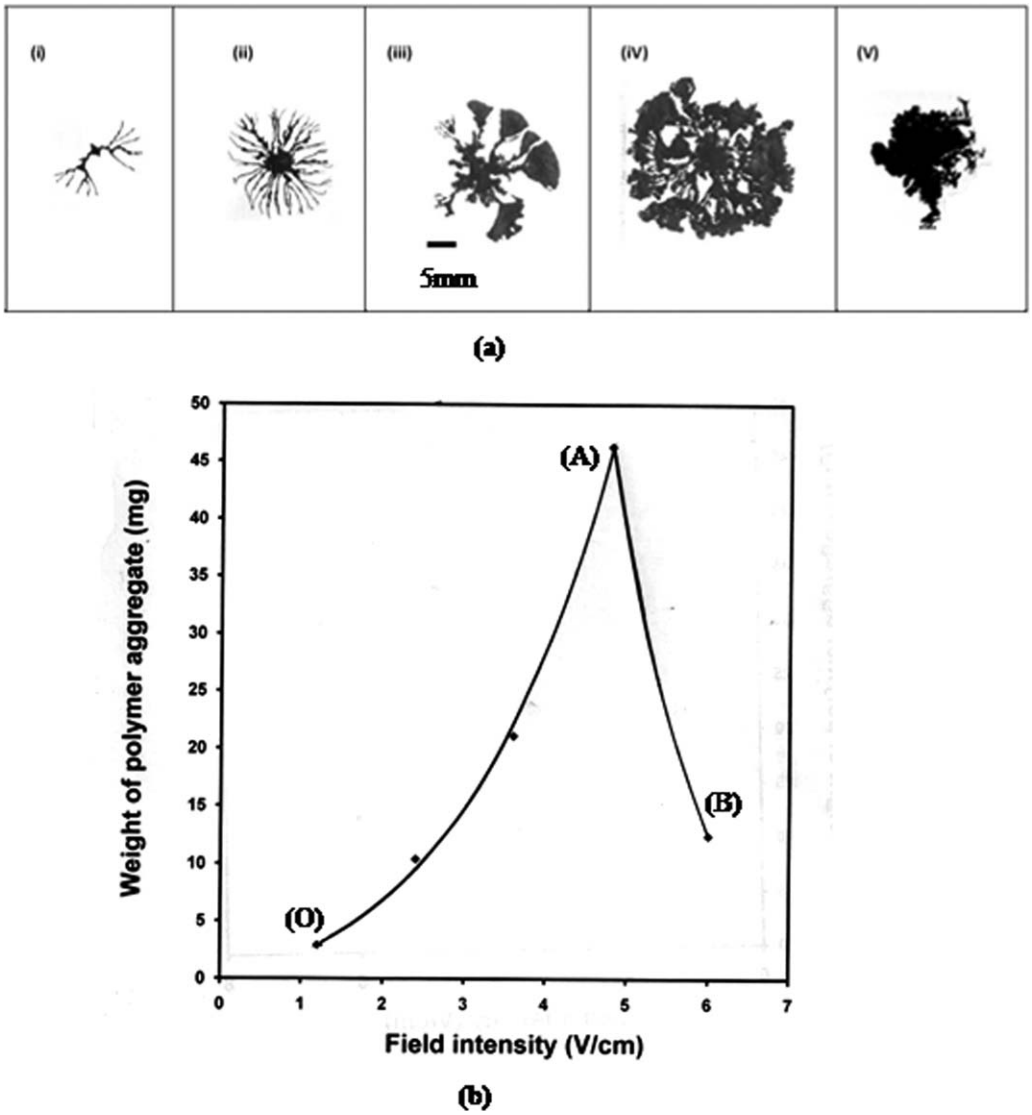

Figure 4. (a) Microphotographs and (b) plot of the weight of the polymer aggregates as a function of the field intensity in the pyrrole–$CuCl_2{\cdot}2H_2O$–NaDS–H_2O system {conditions: [pyrrole] = 0.25*M;* [NaDS] = 0.05*M;* [$CuCl_2{\cdot}2H_2O$] = 0.006*M;* field intensities = (i) 1.2, (ii) 2.4, (iii) 3.6, (iv) 4.8, and (v) 6.0 V/cm; duration of polymerization = 30 min; separation between electrodes = 2.5 cm}.

in earlier studies.[27] Irregular complex aggregates were deposited at the tip of the vertical anode. The experiment was performed at different times, field intensities, and $CuCl_2$ concentrations. The weight of the polymer aggregate was measured at different times with the other parameters fixed. It increased nonlinearly with time, as shown in Figure 1. The growth kinetics were also studied by variation of the field intensity and $CuCl_2$ concentration, as shown in Figures 2 and 3. In system A, initially there was a sharp increase in the weight with increasing field intensity or increasing $CuCl_2$ concentration up to a critical value *B* (Figures 2 and 3), above which there was a decrease in the weight of the polymer in each case. To confirm the previous observations, the electrical conductivity of the solid polymer was measured; it followed the same trend, and the critical value was obtained at *B′* in each case. This indicated that the entire process involved processes of polymerization and degradation of the polymer beyond the critical value *B* or *B′* (Figures 2 and 3). The process of degradation may have taken place because of the decrease in π conjugation of the growing polymer chain.

Electropolymerization proceeded through successive electrochemical and chemical steps. This included the oxidation of the monomer pyrrole to form a radical cation. When current was passed through the system, a pyrrole free-radical cation was formed with the release of one electron. The cation radical thus obtained was stabilized further by resonance as shown here:

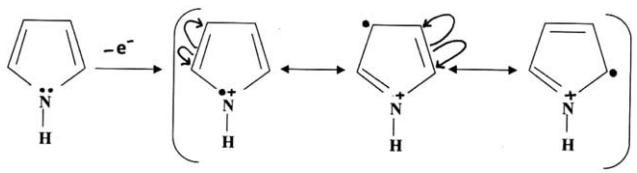

The electron thus released was associated with Cu^{2+} from $CuCl_2$ to form Cu metal deposited at the cathode.

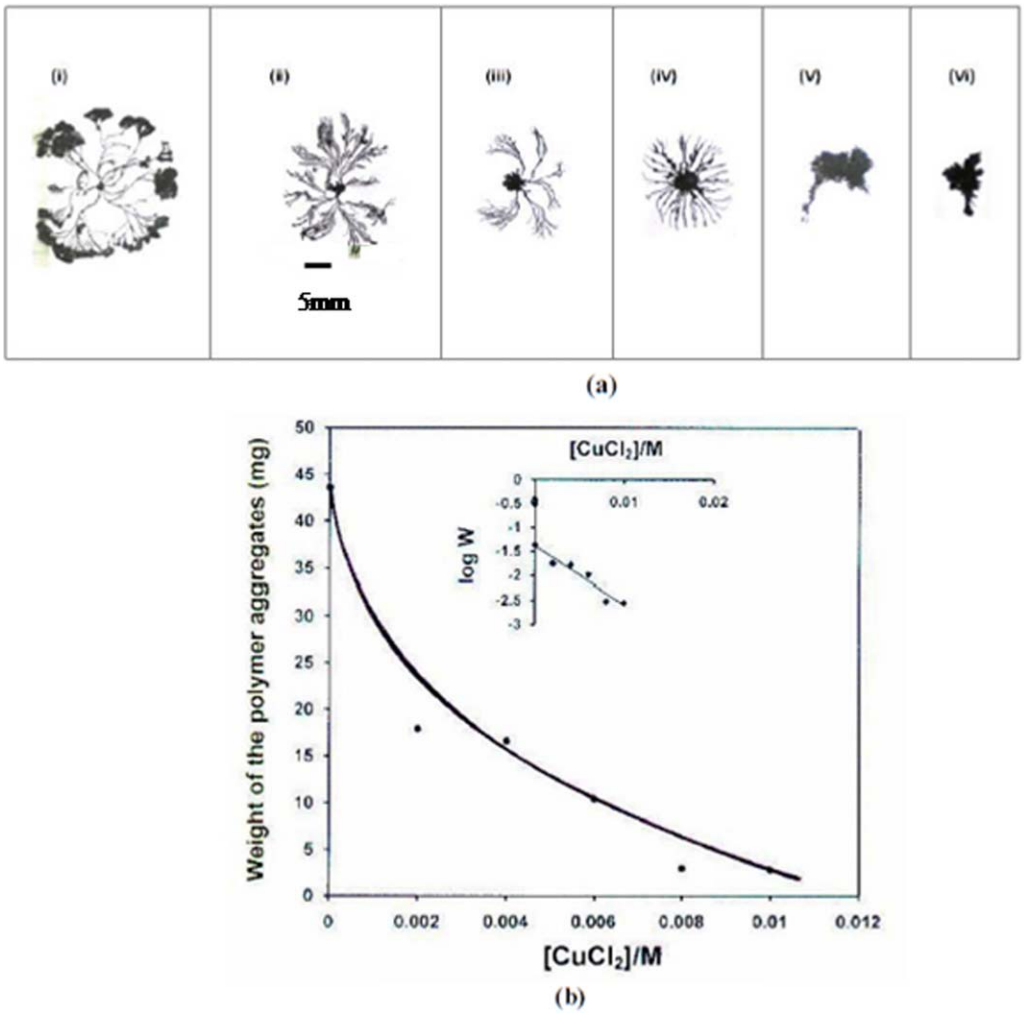

Figure 5. (a) Microphotographs and (b) plots of the weight of the polymer aggregates and (inset) logarithm of the weight of the polymer aggregates (W) as a function of the $CuCl_2$ concentration for the pyrrole–$CuCl_2{\cdot}2H_2O$–NaDS–H_2O system {conditions: [pyrrole] = 0.25*M;* [NaDS] = 0.05*M;* [$CuCl_2{\cdot}2H_2O$] = (i) 0, (ii) 0.002, (iii) 0.004, (iv) 0.006, (v) 0.008, and (vi) 0.01*M;* field intensity = 2.4 V/cm; duration of polymerization = 30 min; separation between electrodes = 2.5 cm}.

$Cu^{2+} + 2e^- \rightarrow Cu$ (deposited at the cathode)

The coupling of two generated radical cations then produced a dimer:

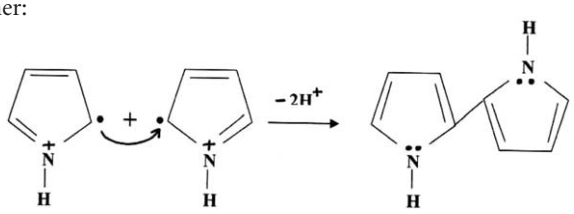

The process was repeated again and again with attack at the α and β positions to form the polymer.

To study the influence of an anionic surfactant on the morphology and growth behavior, NaDS was added to an aqueous solution of pyrrole–$CuCl_2$ (system A), and experiments were carried out at different field intensities and $CuCl_2$ concentrations. The results are shown in Figures 4 and 5. The electrochemical method ensured morphological control. In the presence of NaDS, morphological transitions, as shown in Figure 4, were observed. Irregular, fractal, and dendrimer patterns were obtained; these depended on the field intensity. We also studied the growth behavior by noting the weight of the aggregate as a function of the field intensity. Initially, there was a sharp increase in the weight with an increase in the field intensity,

Table I. *D* Values of the Polymer Aggregates Obtained from the Pyrrole–NaDS–$CuCl_2{\cdot}2H_2O$–H_2O System

[Pyrrole] (*M*)	[$CuCl_2{\cdot}2H_2O$] (*M*)	[NaDS] (*M*)	Field intensity (V/cm)	*D*
0.25	0.006	0.05	2.4	1.20
0.25	0.006	0.05	3.6	1.42
0.25	0.006	0.05	4.8	1.50
0.25	0	0.05	2.4	1.43
0.25	0.002	0.05	2.4	1.25
0.25	0.006	0.05	2.4	1.20

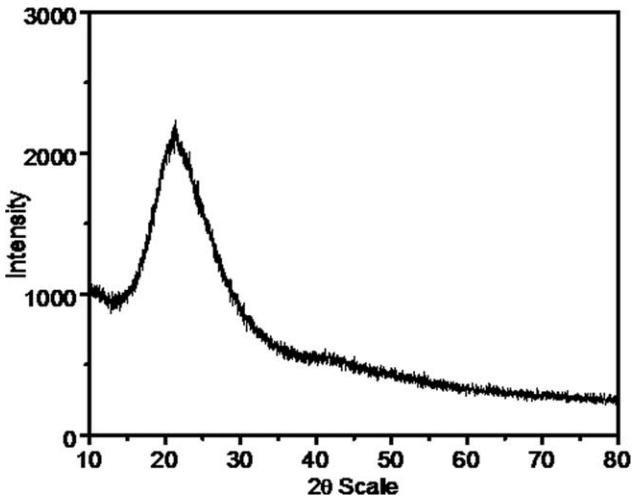

Figure 6. X-ray diffraction pattern of the polymer aggregate obtained from the pyrrole–$CuCl_2{\cdot}2H_2O$–H_2O system (conditions: [pyrrole] = 0.25*M*; [$CuCl_2{\cdot}2H_2O$] = 0.025*M*; field intensity = 2.4 V/cm; time of polymerization = 30 min).

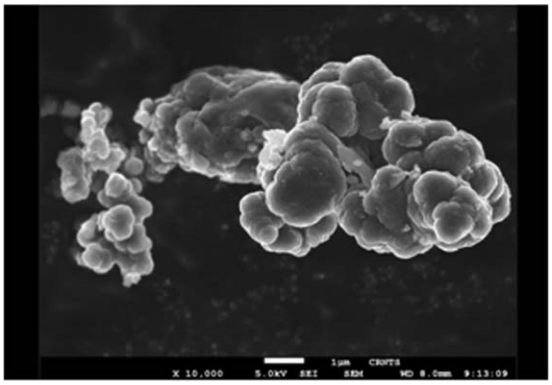

(A)

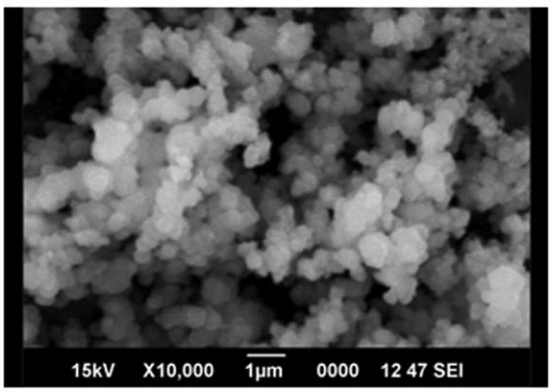

(B)

Figure 7. SEM images of the electropolymerized aggregates obtained from systems A and B (conditions: [pyrrole] = 0.25*M* and [$CuCl_2{\cdot}2H_2O$] = 0.025*M* for system A; [pyrrole] = 0.25*M*, [$CuCl_2{\cdot}2H_2O$] = 0.004*M*, and [NaDS] = 0.05*M* for system B; field intensity = 2.4 V/cm; time of polymerization = 30 min).

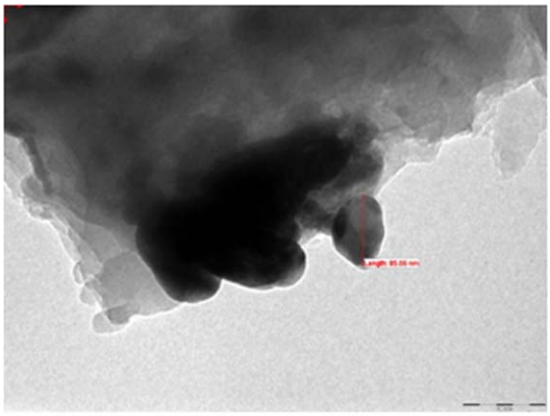

(A)

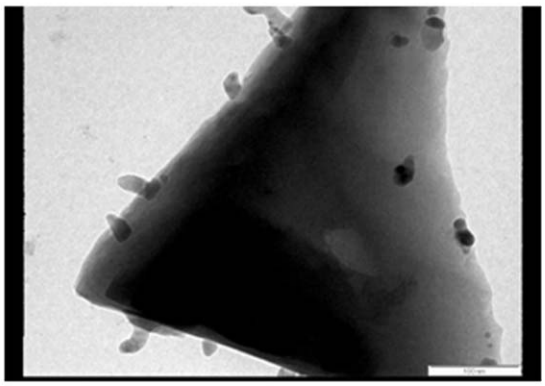

(B)

Figure 8. TEM images of the electropolymerized aggregates obtained from systems A and B (see Figure 7 for the conditions). [Color figure can be viewed in the online issue, which is available at wileyonlinelibrary.com.]

and a critical value at 4.8 V/cm was attained, as shown in Figure 4(b) (point A). Beyond this point, it decreased sharply because of the degradation of the polymer chain. Morphological transitions and growth behavior were also studied at different $CuCl_2$ concentrations, with the other parameters kept fixed. The results are shown in Figure 5. Transitions from dendrimer to fractal and fractal to compact were observed; these depended on the $CuCl_2$ concentration [Figure 5(a)]. The weight of the polymer (W) decreased exponentially with the $CuCl_2$ concentration and obeyed an empirical equation ($w = ce^{m[CuCl2]}$) (where *c* and *m* are intercept and slope respectively), as evident by the straight line obtained between log *w* and the $CuCl_2$ concentration, as shown in Figure 5(b).

The *D* values of the fractal patterns were calculated by a box-counting method. The values of *D* of the patterns are recorded in Table I. The values were accordingly close to the theoretical values of diffusion-limited aggregation. *D* was found to increase with increasing field intensity in the region 2.4–4.8 V/cm and to decrease with increasing concentration of $CuCl_2$.

The X-ray diffraction pattern of the polymer aggregate obtained from system A is presented in Figure 6. It showed only one

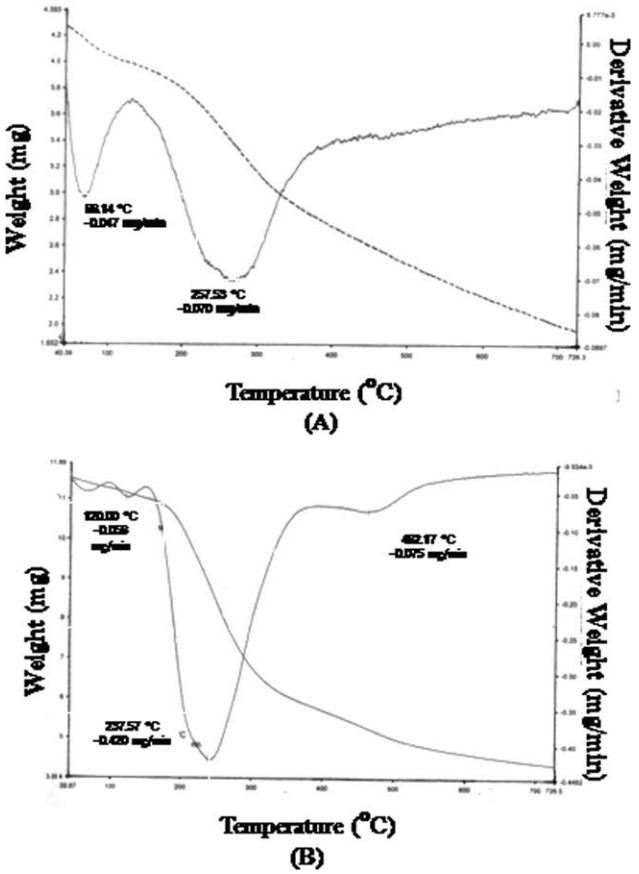

Figure 9. TG/DTG curves for the electropolymerized aggregates obtained from systems A and B (conditions: [pyrrole] = 0.25*M* and [$CuCl_2{\cdot}2H_2O$] = 0.025*M* for system A; [pyrrole] = 0.25*M*, [$CuCl_2{\cdot}2H_2O$] = 0.002*M*, and [NaDS] = 0.05*M* for system B; field intensity = 2.4 V/cm; time of polymerization = 30 min).

peak centered at $2\theta = 23°$, which was characteristic of PPy. No any other peak was seen.

The morphological properties were studied by the SEM and TEM techniques. SEM studies revealed the formation of a classical cauliflower-like aggregate of about 1 μm [Figure 7(A)]. On addition of the anionic surfactant NaDS, the size was reduced, and the shape was changed to a globular structure [Figure 7(B)]. TEM studies [Figure 8(A)] indicated the formation of nanosized spherical particles with sizes of 85 nm for system A and 5–10 nm for system B [Figure 8(B)].

The thermal stabilities of the polymer samples were studied. Thermograms for systems A and B are shown in Figure 9. Weight losses of 53.23 and 63% at 726.5°C were observed for the samples obtained from systems A and B, respectively. The corresponding DTG curves are also shown in Figure 9. We observed that the polymer obtained with $CuCl_2$ alone had a higher stability compared to that obtained in the presence of NaDS.

The IR spectra of PPy prepared with $CuCl_2$ and NaDS were recorded in the region 4000–600 cm^{-1}. The band at 1556 cm^{-1} in the spectrum of PPy–$SO_3C_{12}H_{25}$ corresponded to the C—C stretching vibrations in the pyrrole ring. A redshift to 1540 cm^{-1} of this band was observed in PPy–Cl. The skeletal vibrations, involving the delocalized π electrons, were affected by the doping of the polymer.[8] The most significant feature reflecting the doping process was the appearance of a broad absorption band above 2000 cm^{-1}; this was attributed to an intrachain (free-carrier) excitation.

The bands at 1476 and 1460 cm^{-1} in the spectra of PPy–$SO_3C_{12}H_{25}$ and PPy–Cl, respectively corresponded to C—N stretching vibrations in the ring. The broad band from 1400 to 1250 cm^{-1} was attributed to the C—H or C—N in-plane deformation modes and showed a maximum at 1290 cm^{-1} for PPy–$SO_3C_{12}H_{25}$. This maximum shifted to 1310 cm^{-1} for PPy–Cl. The difference in the spectra of the PPy–$SO_3C_{12}H_{25}$ and PPy–Cl samples was also found in the region from 1250 to 1100 cm^{-1}; this corresponded to breathing vibrations of the pyrrole ring. The maximum was situated at about 1160 cm^{-1} in PPy–Cl and 1197 cm^{-1} in PPy–$SO_3C_{12}H_{25}$. The peak of the S=O stretching vibrations of sulfonate anion was observed at 1184 cm^{-1} in the spectrum of PPy–$SO_3C_{12}H_{25}$. The band of C—H and N—H out-of-plane deformation vibration was situated at 1050 cm^{-1}, and the band of C—C out-of-plane ring deformation vibration was at 970 cm^{-1} for both samples, whereas the band of C—H out-of-plane deformation vibration of the ring had a maximum at 915–920 cm^{-1} for both samples. The peaks at 796 cm^{-1} (C—H out-of-plane ring deformation) and 680 cm^{-1} (C—C out-of-plane ring deformation or C—H rocking) were situated at the same position in the spectra. In both the cases, the formation of PPy was established by IR spectral studies.

The mechanical properties and surface smoothness of the PPy prepared from the aqueous solutions with the addition of the anionic surfactants (system B) were greatly improved in comparison with those of the PPy prepared from the aqueous

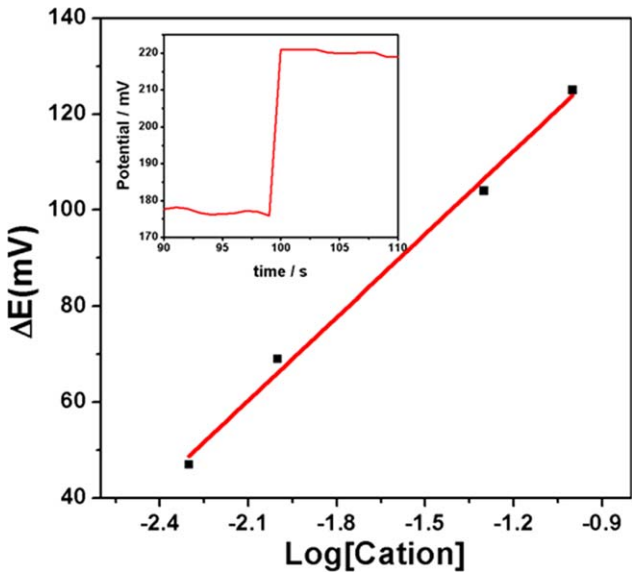

Figure 10. Response curve of the ion sensor to K^+ in 0.1*M* Tris–HCl buffer (pH 7.0) potential difference is plotted against logarithm of cation concentration. (Inset) Typical potentiometric response of a solid-state ion sensor made from a PPy-modified electrode is shown. [Color figure can be viewed in the online issue, which is available at wileyonlinelibrary.com.]

solutions in the absence of surfactant (system A). Accordingly, the typical application of the PPy-modified electrode made with the addition of the anionic surfactant (system B) was used for the development of a solid-state ion-selective electrode. A potassium-ion-selective electrode was constructed on the basis of a dibenzo-18-crown-6 impregnated PVC matrix membrane over the as-synthesized polymer-modified electrode. The electrode showed Nernstian behavior with a slope of 57 mV; this revealed the potential application of the synthesized material in the design of a solid-state ion-selective electrode. A number of experiments were performed over different numbers of days to examine the variation in the baseline recovery during subsequent measurements. The open-circuit potential was found to be on the order of 180 ± 5 mV even after prolonged operation of the solid-state neutral carrier based ion-selective electrode. This justified the potential application of the PPy film for the construction of solid-state ion sensors suitable for practical applications. The typical potentiometric response of the solid-state ion sensor on the addition of various concentrations of K^+ is shown in Figure 10. The response was very fast, with an improved detection limit. The response of the ion sensor was highly selective to K^+.

CONCLUSIONS

In summary, we successfully polymerized pyrrole electrochemically with a copper salt. The influence of an anionic surfactant, NaDS, on the morphology and growth behavior was studied. Polymer aggregates were characterized by powder X-ray diffraction, SEM, TEM, TG/DTG, and Fourier transform infrared studies. The powder X-ray diffraction pattern showed only one peak characteristic of PPy. *D*s of the fractal patterns were calculated. The values were found to be close to the theoretical value of diffusion-limited aggregation. Various morphological transitions, namely, dendrimer to fractal to compact, were observed by changes in the cupric chloride concentration. TEM studies revealed the formation of nanosized spherical particles in the size range 5–10 nm. The thermal stability of the polymer aggregate obtained from system A was higher than that of the aggregate obtained from system B. The application of PPy in the construction of a K^+ selective electrode was described. The ion sensor was highly selective to K^+ with extended linearity over almost 6 decades.

ACKNOWLEDGMENTS

The authors gratefully acknowledge the laboratory facilities provided by the Department of Chemistry of Deen Dayal Upadhyay Gorakhpur University (Gorakhpur, India) and IIT Banaras Hindu University (Varanasi, India). Thanks are due to Pranav Agrawal (United States) and Digvijay Pandey (IIT Banaras Hindu University) for helpful suggestions during the preparation of this article and to the authorities of National Institute of Pharmaceutical Education and Research, Mohali, IIT Bombay, STIC Cochin, and IIT Delhi for help with the analysis.

REFERENCES

1. Rodriguez, J.; Grande, H. J.; Otero, T. F. In Handbook of Organic Conductive Molecules and Polymers; Nalwa, H. S., Ed.; Wiley: New York, **1997**; Vol. *2*, Chapter 10.
2. Qui, Y. J.; Reynolds, J. R. *J. Polym. Sci. Part A: Polym. Chem.* **1992**, *30*, 1315.
3. Liu, Y.-C.; Chung, K.-C. *Synth. Met.* **2003**, *139*, 277.
4. Kuwabata, S.; Nakamura, J.; Yoneyama, H. *J. Chem. Soc. Chem. Commun.* **1988**,*12*, 779.
5. Zhang, L. J.; Wan, M. X. *Adv. Funct. Mater.* **2003**, *13*, 815.
6. Dai, T.; Yang, X.; Lu, Y. *Nanotechnology* **2006**, *17*, 3028.
7. Xi, S.; Zhao, G. *J. Appl. Polym. Sci.* **2007**, *104*, 1987.
8. Omastova, M.; Trchova, M.; Kovarova, J.; Stejskal, J. *Synth. Met.* **2003**, *138*, 447.
9. Zhang, X.; Zhang, J.; Song, W.; Liu, Z. *J. Phys. Chem. B* **2006**, *10*, 1158.
10. Selvan, S. T. *Chem. Commun.* **1998**, *3*, 351.
11. Xiaofun, Y.; Lingge, Xu.; Choon, N. S.; Hardy, C. S. *Nanotechnology* **2003**, *14*, 624.
12. Chen, C.; Fu, X.; Fan, W.; Ma, T.; Wang, Z.; Miao, S. *Mater. Lett.* **2015**, *138*, 279.
13. Liu, P.; Huang, Y.; Zhang, X. *Mater. Lett.* **2014**, *136*, 298.
14. Samuelson, L. A.; Druy, M. A. *Macromolecules* **1986**, *19*, 824.
15. Pina, C. D.; Falleta, E.; Rossi, M. *Catal. Today* **2011**, *160*, 11.
16. Ben-Jacob, E.; Garik, P. *Nature* **1990**, *343*, 523.
17. Nakanishi, S.; Nagai, T.; Fukami, K.; Sonoda, K.; Oka, N.; Ihara, D.; Nakato, Y. *Langmuir* **2008**, *24*, 2564.
18. Fleury, V. *Nature* **1997**, *390*, 145.
19. Rastogi, R. P.; Das, I.; Pushkarna, A.; Sharma, A.; Jaiswal, K.; Chand, S. *J. Chem. Educ. A* **1992**, *69*, 47.
20. Rastogi, R. P.; Das, I.; Jaiswal, K.; Chand, S. *Ind. J. Chem. A* **1993**, *32*, 749.
21. Das, I.; Choudhary, R.; Kumar, S.; Agrawal, P. *J. Phys. Chem. B* **2011**, *115*, 8724.
22. Daccord, G.; Lenormand, R. *Nature* **1987**, *325*, 41.
23. Fujikawa, H.; Matsushita, M. *J. Phys. Soc. Jpn.* **1989**, *58*, 3875.
24. Ben-Jacob, E.; Schochet, D.; Tenenbaum, A.; Cohen, I.; Czerok, A.; Vicsek, T. *Fractals* **1994**, *2*, 15.
25. Das, I.; Kumar, A.; Singh, U. K. *Ind. J. Chem. A* **1997**, *36*, 1018.
26. Pandey, P. C.; Prakash, R. *Sens. Actuators B* **1998**, *46*, 61.
27. Das, I.; Agrawal, N. R.; Gupta, S. K.; Gupta, S. K.; Rastogi, R. P. *J. Phys. Chem. A* **2009**, *113*, 5296.